*Tiffany M. Addington*[1], *John S. Scheibe*[1],
*Arron J. Hendershott*[2]

# Planar Surface Area and Launch Performance in *Glaucomys volans*

*Abstract*

*We used still photography and high speed strobes to investigate planar surface area and patagial shape during laboratory launches by Glaucomys volans. Planar surface area increased throughout the launch sequence to a maximum of 196 cm$^2$ at 0.333 s. Launch velocity was positively correlated with planar surface area, while animal mass was negatively correlated. The lift coefficient was initially high, but a projection for mid-glide produced values consistent with previously reported values for other species. However, Glaucomys appears to have relatively high lift coefficients. Patagial shape is dynamic during the launch, and reveals pronounced changes during turns. Preliminary analysis using thin-plate splines reveals no consistent patagial shape changes during left or right turns at low speeds associated with the launch, but there is change in the shape of the wingtip.*

*Keywords*

*Glaucomys, planar area, lift, launching*

## 1. Introduction

There have been few studies of gliding performance in mammals [2, 3, 10, 11, 13, 18]. Robins [14] analyzed more than 100 glides by *Glaucomys volans,* and explored the relationship between morphology and performance. Scheibe and

1 Department of Biology, Southeast Missouri State University, Cape Girardeau, MO 63701 USA.

2 Missouri Department of Conservation, Cape Girardeau, MO 63701 USA.

Robins [17] performed additional analyses for this species, and used the model of Scholey [18] to explore the cost of gliding transport relative to quadrupedal transport. Keith et al. [6] investigated launch dynamics in *G. volans* and determined that leaping launches add little to the energetic cost of gliding. These studies demonstrate that *G. volans* has a typical glide ratio of about 1.53 (≅ 33.2°), its terminal glide speed is about 8.27 m/s, and it must travel about 5 m before gliding is energetically less expensive than quadrupedal transport. These findings are consistent with the review of Dolan and Carter [5] who report *G. volans* gliding 30 m or more, but generally restricting glides to 6–9 m.

Performance studies by Nachtigall [10] and Nachtigall et al. [11] on the marsupial sugar glider, *Petaurus breviceps*, and by Polyokova and Sokolov [13] on the pteromyine *Pteromys volans* are generally consistent with the performance data reported above for *G. volans*. Nachtigall et al. [11] used a wind tunnel in their analysis of gliding, and reported glide angles of about 27° for *P. breviceps*. They estimated lift coefficients and glide polars. No lift coefficients have been reported for *G. volans*.

Thorington and Heaney [20] analyzed body proportions of gliding squirrels, and determined that in general, pteromyines are more gracile than non-gliders. Presumably this increases patagial surface area, providing greater lift coefficients for gliding. Flying squirrels have lower aspect ratio wings, and lower glide ratios than hang gliders, but function in a similar fashion [20]. Analyses and descriptions of wing loading in gliding mammals have necessarily assumed a static patagium. Patagial surface areas have been estimated from dry museum skins, or from skeletal material. At the same time, observations of flying squirrels show them to be extremely maneuverable while gliding. We have observed complete rolls and 180° turns. This maneuverability suggests considerable postural control of the glide trajectory, and illustrates the dynamic nature of the patagium.

In this paper, we investigate changes in patagial surface area during launches by *G. volans*. We show the surface area to be dynamic, resulting in changes in lift and drag as the animal follows its initial ballistic path. These results add to our understanding of gliding in *G. volans*, and provide a first step in a complete description of gliding by this species.

## 2. Methods

A laboratory colony of approximately 15 *Glaucomys volans* (Sciuridae; Pteromyinae) was established in 1985. The animals were captured in the Kelso Wildlife Sanctuary, Cape Girardeau Co., MO. Most animals in the colony were wild caught, although several were born in captivity. The animals were maintained in two indoor enclosures each measuring 2.5 × 1.5 × 2.4 m. The enclosures were large enough to permit leaping and short glides, as well as establishment of typical social hierarchies [7, 8, 9, 19]. Animals were maintained on a diet of pecans, walnuts, peanuts, sunflower seeds, and birdseed. Food and water were provided ad lib., with occasional supplementary vitamins.

The temperature-regulated room was maintained on a consistent 12 h L/D photoperiod. Access to the colony was restricted to minimize disturbance of the animals.

All gliding trials were conducted in a 7 × 14 m lab with a 7 m ceiling (described in [6]). Two 3.5 m snags were erected in the lab, and served as launching and landing posts. A 0.5 m section of 3.18 cm dowel rod was attached to the top of one snag, and served as a launching 'branch.' A black 3.7 × 5.5 m canvas tarp was suspended from the ceiling to provide a high contrast background for ventral views of the squirrels. An infrared shutter-beam (Woods Electronics Inc., Poway, CA 92064, USA) was used to direct an infrared beam across the top of the launch branch. The shutter-beam was attached to two Canon 540ez high-speed strobes. One strobe was attached to the side of the launch snag and illuminated the ventral surface of the animal. The second strobe illuminated the lateral surface of the animals. When the infrared beam was interrupted by a squirrel, the strobes fired at 12 hz for 0.7 s.

Three 35 mm still cameras were used to capture stroboscopic images of the launching squirrels. A Canon A2E was attached to the strobes, with its shutter opening just prior to the first strobe burst, and closing following the final strobe burst. Two additional cameras were operated manually. Shutters on these cameras were opened manually in the darkened lab, and closed when the strobes ceased firing.

The Canon camera was mounted on a tripod directly between the snags, and was aimed upward to capture the dowel rod, a ventral view of the launching squirrels, and the black canvas background. When the animals launched, this camera captured multiple images of the ventrum of a squirrel, leaping away from the dowel rod (Fig. 1). A second camera was positioned to capture a lateral view of the entire launch sequence, and a third camera was used to capture a close-up lateral view of each launch. Images from these cameras were used to corroborate vertical position of the animals. Since the strobes fired at 12 hz, each negative contained an image of a launching squirrel at 0.083 s, 0.167 s, 0.25 s, and 0.333 s after the infrared beam was interrupted. This strobe frequency resulted in no overlap between successive images of the launching squirrels. A higher frequency would have resulted in negatives with overlapping images of launching squirrels, and made estimation of planar surface area difficult. Lower frequencies would have reduced the number of useable images.

Kodak Plus-X film was used throughout the study. Film was developed in Kodak D76 developer. Negatives were digitized by placing them on a light table, and filming them with an 8 mm video-recorder mounted on a copystand. A Minolta Snappy frame grabber was then used to capture the images for computer analysis. The images were analyzed using SigmaScan (SPSS Inc., 444 N. Michigan Ave., Chicago, IL 60611, USA). Images of the ventral surface were analyzed separately from lateral views. Negatives of ventral views were calibrated using previously determined hind foot measurements. Contrast of each negative was then maximized within SigmaScan, resulting in a white squirrel

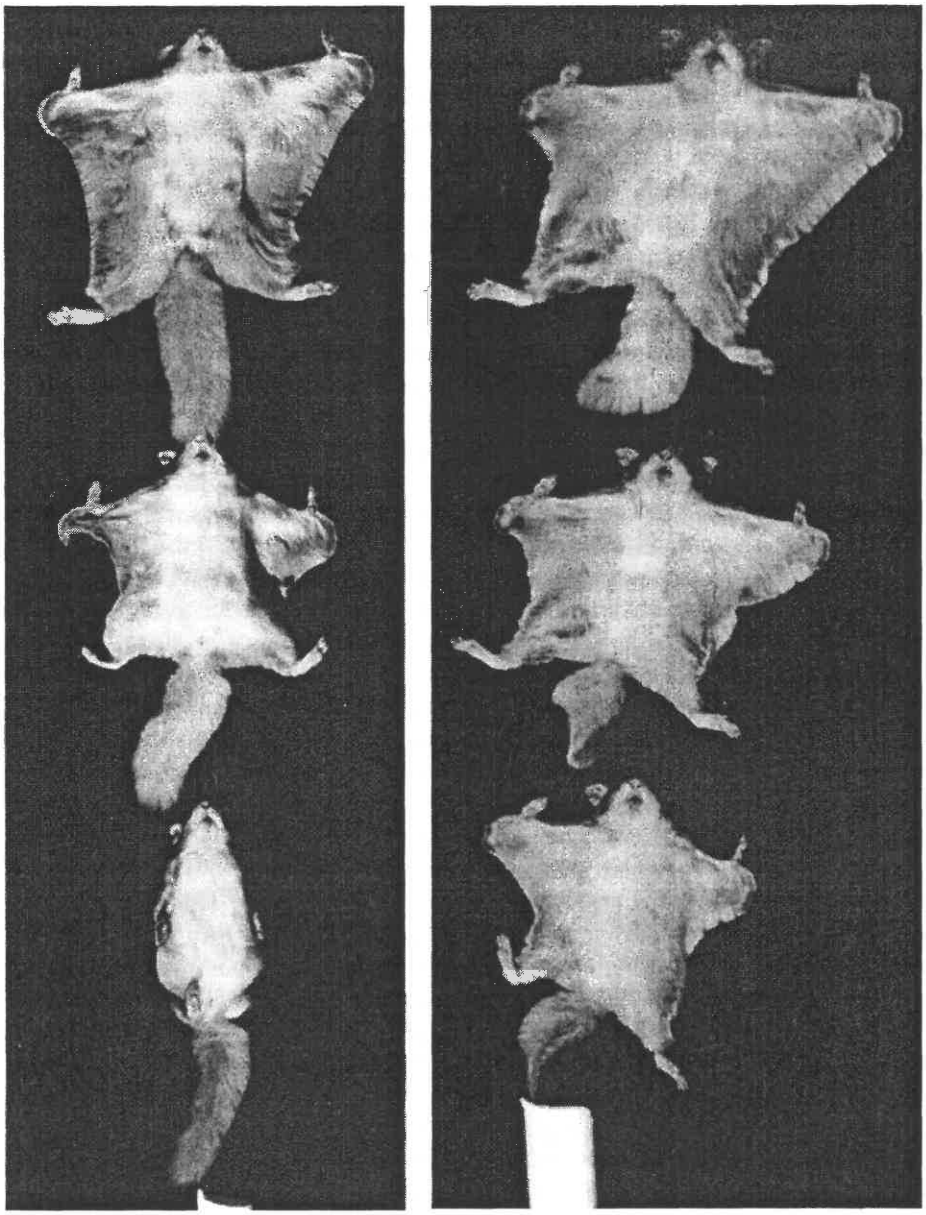

**Fig. 1.** Multiple images of a leaping *Glaucomys volans*.

image against a black background. The ventral planar surface area of the animal was then measured at each point along its launch trajectory. Negatives of lateral views were calibrated using the diameter of the dowel rod. For these

images, a clearly identifiable landmark such as the tip of the rostrum or eye was chosen on each squirrel. Coordinates for these points were then established within SigmaScan, and exported to QuatroPro for analysis. These coordinates were then used to determine launch angle and launch velocity. Regression results from Keith et al. [6] were used to estimate launch trajectories and glide angles.

Changes in patagial surface area were related to overall estimates of glide parameters based on the work of Keith et al. [6]. Our estimates of launch angle were used to estimate glide angles using the regression $\alpha_g = 36.073 - 0.702\ a_L$ where $\alpha_g$ is the glide angle and $\alpha_L$ is the launch angle. The horizontal and vertical position of the squirrel at any time during its trajectory was estimated using regression equations derived from work by Keith et al. [6]. Here,

$$X = -0.18999 + 185.3076T + 145.6148T^2$$

and

$$Y = -0.085 + 61.48737T - 325.558T^2,$$

where X and Y are the horizontal and vertical positions of the squirrel relative to its launch point, and T is time in seconds since initiation of the launch. Thus, at each time it was possible to estimate the animal's position, and by computing the first derivative, horizontal, vertical, and total velocity. The second derivative provided acceleration at each time.

Estimated mean velocities at 4 points along the trajectory (0.083 s, 0.167 s, 0.25 s, 0.333 s) were correlated with mean planar surface areas at those times. Planar surface area at 0.25 s was correlated with animal mass and an index of glide angle using Pearson product moment correlations. Surface area at 0.25 s was used because not all negatives contained an image of a flying squirrel at 0.333 s, and we were interested in the largest possible airfoil. We estimated glide angle using the regressions of Keith et al. [6] for horizontal and vertical position against time. We used the cosine of horizontal distance over vertical distance traveled during each 0.0 8 3s time interval.

The coefficient of lift was estimated at 4 points along the glide trajectory using $C_L = 2N \cos \alpha_g / rV_g^2$ where N is wing loading, r is air density (estimated as 1.22 $kg/m^3$), and $V_g$ is glide velocity [18]. Coefficient of lift was correlated with planar surface area using a Pearson product moment correlation.

Patagial shape during turns was investigated using thin-plate splines [4]. We chose 13 landmarks (Fig. 2) as follows: 1) tip of tail, 2) base of tail, 3) toe of right hind foot, 4) heel of right hind foot, 5) tip of right forefoot, 6) heel of right forefoot, 7) tip of right styliform cartilage, 8) tip of rostrum, 9) tip of left forefoot, 10) heel of left forefoot, 11) tip of left styliform cartilage, 12) toe of left hind foot, and 13) heel of left hind foot. Because of postural variation from launch to launch, no effort was made to estimate a mean shape. Instead, we chose two ventral views of launches which illustrated clear turns to the left, two views which illustrated clear turns to right, and one view which was relatively

straight. During the course of the study, many animals turned left or right and avoided the landing snag. These turns were assumed to represent natural turns. Coordinates of each image were determined using SigmaScan, and exported to QuatroPro. The coordinates were standardized by assigning (0,0) to landmark 2, and (1,0) to landmark 8. All remaining landmarks were re-scaled and aligned to match the reference coordinates. Principal warps were computed for the animal 0.83 s after launch using TpSpline 1.02 (Michigan Morphometrics Workshop: www.life.bio.sunysb.edu/morph/). This reference shape was then compared with the ventral view of the same animal 0.167 s later. The animal at 0.167 s was then used as the reference shape and compared to the same animal at 0.25 s. If a fourth stroboscopic image was present, the shape at 0.25 s was compared to the final shape at 0.333 s. We made no attempt to explore partial warps, and investigated only total splines.

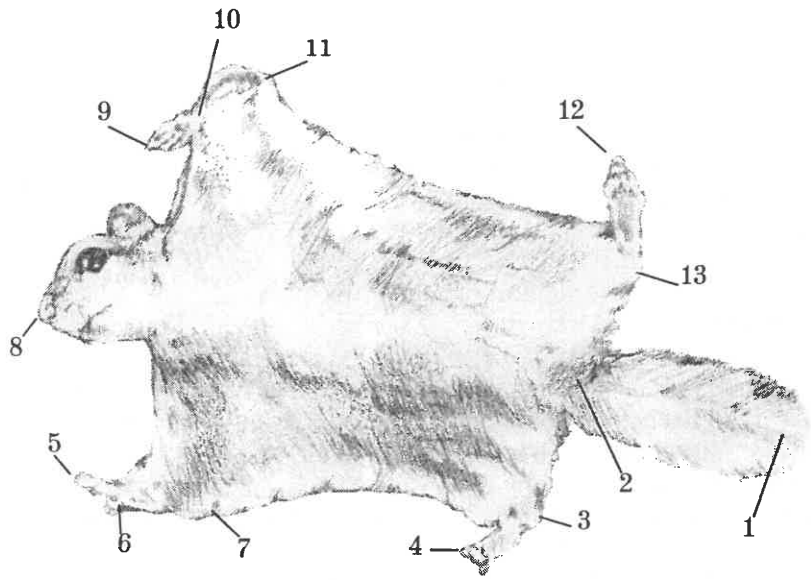


**Fig. 2.** Ventral view of a launching *Glaucomys volans*. Landmarks are: 1) tip of tail, 2) base of tail, 3) tip of right hindfoot, 4) heel of right hindfoot, 5) tip of right forefoot, 6) heel of right forefoot, 7) tip of right styliform cartilage, 8) tip of snout, 9) tip of left forefoot, 10) heel of left forefoot, 11) tip of left styliform cartilage, 12) tip of left hindfoot, heel of left hindfoot.

## 3. Results

Stroboscopic images of the ventral surface of launching *G. volans* revealed features of the launch that have not been reported. Within each 0.083 s interval, the animals exhibited extensive postural changes. Hind and forefeet, limbs,

and tail often changed position and orientation, suggesting the animals exerted control over their glide paths.

As noted by Keith et al. [6], tail position was stereotypical during the first moments of launch. It was laid over the dorsal aspect of the animal during the leap, and laid back as an apparent airfoil during the glide. Our images showed the tail was often turned for short intervals so that it appeared much like a rudder on an airplane. During contact with the launch platform, the digits of the hind feet faced anteriorly. However, within 0.083 s they were turned outward, but moved forwards and backwards without apparent synchrony. At 0.333 s movement of the rear feet had stopped, the plantar surface faced down and back, with some plantar extension. The fore feet were oriented so that the digits faced forwards throughout the launch sequence. At 0.083 s the forelimbs were not fully extended, but were wider than the hind limbs. The styliform cartilage was erected by 0.167 s. The margin of the patagium was usually not completely taut until about 0.333 s into the glide. At 0.083 s, the animals appeared much like a mouse leaping from a branch, with the forelimbs moved forward and the hind limbs pushing off from the branch. At 0.167 s the forelimbs were spread, the styliform cartilages erected, and the patagium formed an anterior wing. Generally, at 0.25 s the hind limbs had moved laterally and the patagium formed a trapezoidal airfoil which was wider anteriorly. The trapezoidal shape was maintained at 0.333 s, but increased in surface area and tautness of the patagial margin.

Patagial shape was dynamic during turns. Splines for animals turning right or left revealed no simple modification of wing tip or posture (Fig. 3). Whereas in some cases animals turning right modified the left wing tip and those turning left modified the right wingtip, there was no consistent pattern. Instead, turns appeared to be associated with modifications of the wingtips, patagial margins, tail position, and hand position, at least at the relatively slow velocities associated with launch. Higher velocities during mid-glide may entail more consistent postural changes during turns.

Planar surface area nearly doubled during the first 1/3 second of the launch (Table 1) from 103.92 $cm^2$ (95 % CL: 89.85–117.99) to 196.01 $cm^2$ (95 % CL: 170.92–221.10). There was considerable variation in planar surface area during the launch sequence, which is not surprising in light of the postural changes employed by the animals as they selected their ballistic trajectories and landing sites.

Velocity during the launch phase increased from about 2 m/s at 0.083 s to 2.38 m/s at 0.333 s. Since the animal can accelerate actively only while it has contact with the launch surface, the increased velocity at 0.333 s is a consequence of gravitational acceleration. Planar surface area was positively correlated with velocity ($r = 0.95, p < 0.05$), but negatively correlated with animal mass ($r = -0.39, p < 0.05$). Animals with the greatest velocities had the highest surface areas, but also had lower overall mass. Animals with less mass had higher acceleration during the launch, and the greatest planar surface areas.

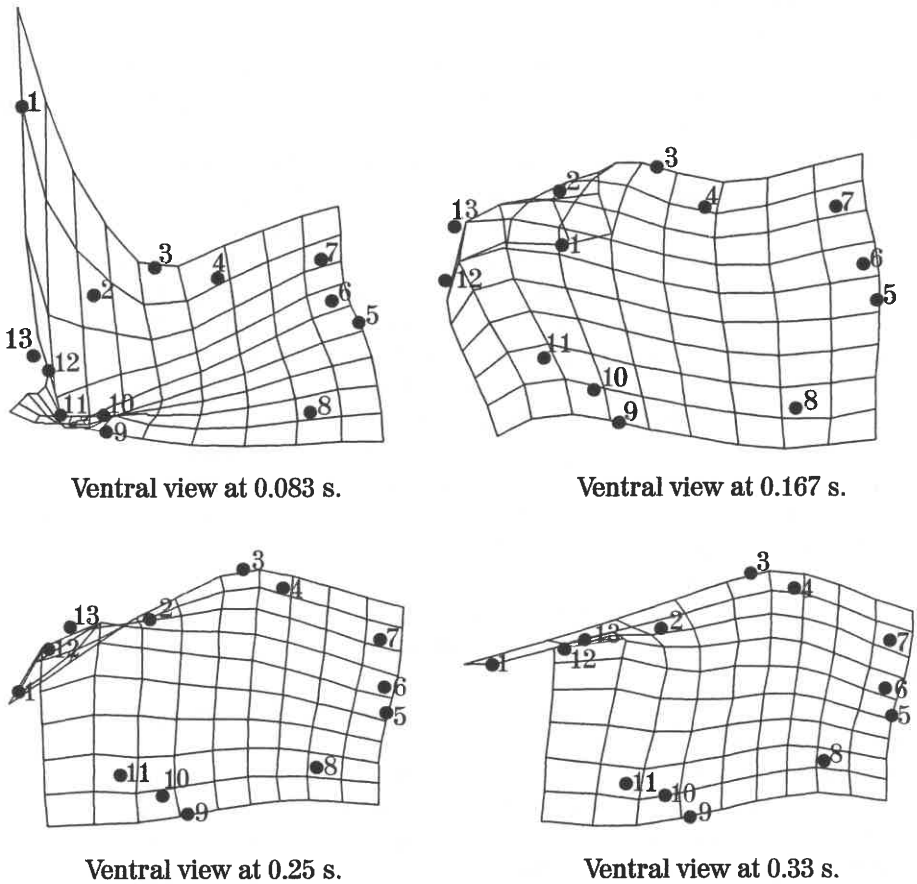


**Fig. 3.** Relative warps of a ventral view of a southern flying squirrel at 4 times during the launch sequence (0.083s, 0.167s, 0.25s, and 0.33s). Landmarks are: 1) tip of tail, 2) base of tail, 3) tip of right hindfoot, 4) heel of right hindfoot, 5) tip of right forefoot, 6) heel of right forefoot, 7) tip of right styliform cartilage, 8) tip of snout, 9) tip of left forefoot, 10) heel of left forefoot, 11) tip of left styliform cartilage, 12)tip of left hindfoot, heel of left hindfoot. The warps illustrate flaring of the styliform cartilages, and rotation of the forefeet.

Planar surface area was not correlated with projected glide angle ($r$ = -0.11, $p > 0.05$), indicating that within the context of short glides, planar surface area at 0.333 s after launch is not a good indicator of ultimate glide performance, and that patagial surface area is more important during later stages of the glide. However, estimates of the coefficient of lift were greatest immediately following launch, and decreased at least through the first 0.333 s (Table 1). This is a consequence of changes in wing loading, glide angle, and glide velocity. Reduced lift coefficients can result from increased glide velocity,

**Table 1**
Parameter estimates at 4 times during glide launch by *Glaucomys volans*.

| Time Since Launch (s) | 0.083 | 0.167 | 0.250 | 0.333 |
|---|---|---|---|---|
| Angle (degrees) | 0.0 | 5.048 | 16.737 | 25.268 |
| Velocity (m/s) | 2.004 | 2.096 | 2.226 | 2.383 |
| Planar Surface Area ($cm^2$) | 103.924 | 146.267 | 181.358 | 196.014 |
| (± 95 % CL) | (14.069) | (9.853) | (11.228) | (25.089) |
| Wing Loading ($N/m^2$) | 73.629 | 52.314 | 42.192 | 39.037 |
| Coefficient of Lift | 30.055 | 19.445 | 13.367 | 10.191 |
| (95 % CL) | (26.5–34.8) | (18.2–20.9) | (12.6–14.3) | (9.0–11.7) |

increased glide angle, or decreased wing loading. The animals accelerated through the launch as a consequence of gravitational acceleration, wing loading decreased as patagial surface area increased, and the glide trajectory deteriorated through early portions of the glide, all contributing to reduced lift coefficients.

## 4. Discussion

Estimates of patagial surface area are usually based on dried museum skins, and consequently have high measurement errors. Robins [14] measured patagial surface area as well as head and tail surface area on 20 anesthetized southern flying squirrels. His estimate of 212.13 $cm^2$ (± 21.53) is larger than our estimate at 0.333 s of 196.01 $cm^2$ (± 25.09). The difference may actually be greater in light of recent work by Thorington et al. [21], who show the styliform cartilage probably requires active erection. However, our animals maintained an angle of attack which was non-zero, and planar surface area should be less than overall patagial surface area. More importantly, our data show planar surface area approaches presumed maximal values reported by Robins [14] within 0.333 s of launch. Thus, *G. volans* seems not to rely on an initial vertical drop for acceleration in early portions of the glide as described by Scholey [18] for *Petaurista petaurista*.

To a large extent, lift is dependent on planar surface area, velocity, and the lift coefficient. During the launch sequence, the lift coefficient decreased from 30.055 to 10.191, while lift decreased from 0.765 N/s to 0.692 N/s. If we assume planar surface area and glide angle at 0.333 s approximate values later in the glide, we can estimate mid-glide lift coefficients. Scheibe and Robins [17] estimated mean glide speeds of about 6.37 m/s, and terminal glide speeds of about 8.27 m/s for *G. volans*. At mean glide speed, the lift coefficient would be between 1.32 and 1.51 at the 9 5% confidence limits for planar surface area. At

the terminal glide speed of 8.27 m/s, the lift coefficient should lie between 0.69 and 0.90. At mean glide speed, estimated values are somewhat higher than the lift coefficient of 0.84 reported by Scholey [18] for *P. petaurista*. Similarly, Nachtigall [10] and Nachtigall et al. [11] reported a lift coefficient of 0.6 for *Petaurus breviceps papuanus*, a subspecies of the marsupial sugar glider that is similar in size to *G. volans*. If these values are accurate and not simply different because of methodology, gliding locomotion in *G. volans* may be fundamentally different from that in *Petaurista* or *Petaurus*. While at terminal glide speed, the lift coefficients for *G. volans* encompass the value reported by Scholey, coefficients at mean glide speed indicate greater maneuverability, and consequently a greater ability to exploit efficiently a complex habitat.

Planar surface area was negatively correlated with mass. Animals with less mass had greater planar surface area and consequently low wing loading. In order to increase the lift coefficient with low wing loading, it is necessary to reduce glide velocity. Interestingly, Keith et al. [6] noted a trend for decreased launch acceleration in smaller *Glaucomys*. Ando and Shiraishi [1] report wing loading in *Petaurista leucogenys* to be 81 N/m$^2$, and Thorington and Heaney [20] note that wing loadings in the Pteromyinae range from perhaps as low as 25, to as high as 110 N/m$^2$. In bats, wing loadings vary from 10–20 N/m$^2$ [20]. Immediately after launch, wing loading in *G. volans* was 73.7 N/ m$^2$ while after 0.333 s it was 39 N/m$^2$.

*Petaurista leucogenys* glides at speeds ranging from 7–13.3 m/s [3], depending on glide ratio (horizontal gliding distance/vertical drop). At glide ratios of about 2 (direct glide angle = 26.565°), glide speeds were about 8.5–11 m/s, while at glide ratios of 3 (direct glide angle = 18.435°) speeds ranged from 9–13.3 m/s. Thus, lift coefficients for *P. leucogenys* should vary from about 0.98–1.64 at a glide ratio of 2, and 0.71–1.56 at a glide ratio of 3. These values are biased since they are based on patagial rather than planar surface area. Values based on planar area should be somewhat higher. At 6.37 m/s, *Glaucomys* has an estimated lift coefficient between 1.32 and 1.51, which is greater than the low-end values for *Petaurista leucogenys*. Ando and Shiraishi [3] note the lack of maneuverability in *P. leucogenys*, which may be explained at least partially by the low lift coefficients at high speeds. The low speeds observed in this study corresponded with high lift coefficients, and a high degree of maneuverability.

*Glaucomys volans* exhibits reverse sexual dimorphism [15]. Females are significantly longer than males but have less mass. Thus, patagial surface area of females is larger than that of males, and wing loading is considerably less. They attributed this difference to reproductive constraints on females. That is, females carry additional mass when pregnant, and are involved in the transport of young weighing as much as 40 g. Interestingly, when they added the mean mass of a near term litter to adult female mass, females were not different from males. This suggests strongly that reduced wing loading in females accommodates reproduction. Furthermore, they found important differences in morphological variance associated with styliform cartilages, limbs, and tails

of adult males and females. There was reverse sexual dimorphism with respect to tail and limb length, and styliform cartilages in females tended to be longer as well. These components are associated with planar area, and the tail and styliform may be critical as rudders and wingtips. It would be interesting to determine how wing loading and other aspects of reverse sexual dimorphism influence gliding performance in *Glaucomys*.

Shape and area of the patagium are dynamic, and change dramatically during the launch sequence. These changes are associated with postural changes, which presumably influence the direction and trajectory of the glide. The tail appears to be important during the launch since it is almost universally laid over the back of the animal during the first 0.25 s. The same pattern appears in *Petaurus breviceps* at launch, and may function either to move the center of mass forward, or to increase the angle of attack by forcing the posterior portion of the animal downward. By 0.333 s, the tail is extended posteriorly and acts as a flow rudder [16], increasing the planar surface area of the animal. The tail operates as a control mechanism for speed and pitch [12]. It is important to note that the tail is distichous and dorso-ventrally flattened, unlike the longer tail in *Petaurus*.

Ando and Shiraishi [3] used cinematography at 18 frames/s and a motor driven still camera at 5 frames/s to capture some images of gliding *P. leucogenys*. Their images reveal significant, rapid postural changes in this relatively large glider. Within 0.13 s of launch, *P. leucogenys* shows a 45° depression of the body axis. At 0.15 s the animals initiated simultaneous extension of the limbs, and at 0.30 s the limbs and styliform cartilages were fully extended. At 0.333 s, depression of the body axis was reduced to 15°.

Some of our launch sequences included animals that did not launch straight forward, but rather turned to the left or right. In some of these images, animals turning left extended the right forelimb at 0.167 s while keeping the left forelimb closer to the body. Thus, the right side of the animal possessed a pronounced wing and wing tip while the left side did not. Similarly, some animals, which turned to the right, extended the left forelimb and wing tip while the right side was less pronounced. However, there was no consistent pattern across the majority of launches, either because of variation between launches or the precise timing of the strobe bursts relative to initiation of the launch. It is apparent that extensive postural changes take place within a fraction of a second, indicating significant behavioral control over the glide.

While hang-gliders may represent a reasonable model for gliding mammals [20], it is clear that gliding involves a complex series of postures. Patagial shape, velocity, planar surface area, and even the wing tip [21] have significant influence over performance. Clearly, launching in *Glaucomys* is not a simple event, and involves postures and consequent aerodynamic changes that require behavioral control. It is unknown how most gliding mammals initiate or control their glides. We have some information for *Petaurus*, *Petaurista*, and *Glaucomys*, but none for any of the other gliders. We don't know if *Glaucomys* has solved the aerodynamic problems associated with gliding in a unique way,

or if all gliders employ the same basic approach. In light of the morphological differences between the marsupials, anomalurids, and pteromyines, we suspect there are important differences.

## Acknowledgements

We thank J. Robins, N. Young, B. Seegers, and M. Keith for their assistance during various stages of the project, and P. Roopnarine for his critical comments on an earlier draft of the manuscript. J. Cross provided the illustration for Figure 1.

### Literature Cited

[1] Ando, M., and S. Shiraishi (1984): Relative growth and gliding adaptations in the Japanese giant flying squirrel, *Petaurista leucogenys*. *Science Bulletin of the Faculty of Agriculture, Kyushu University* 39: 49–57.

[2] Ando, M., and S. Shiraishi (1991): Arboreal quadrupedalism and gliding adaptations in the Japanese giant flying squirrel, *Petaurista leucogenys*. *Honyurui Kagaku (Mammalian Science)* 30: 167–181.

[3] Ando, M., and S. Shiraishi (1993): Gliding flight in the Japanese giant flying squirrel *Petaurista leucogenys*. *Journal of the Mammalogical Society of Japan* 18: 19-32.

[4] Bookstein, F.L., (1989): Principal warps: Thin-plate splines and the decomposition of deformations. *I.E.E.E. Transactions on Pattern Analysis and Machine Intelligence* 11: 567–585.

[5] Dolan, P.G., and D.C. Carter (1977): *Glaucomys volans*. *Mammalian Species* 78: 1–6.

[6] Keith, M.K., J.S. Scheibe, and A.J. Hendershott (this volume): Launch dynamics in *Glaucomys volans*. In: *The Biology of Gliding Mammals* (R.L. Goldingay & J.S. Scheibe, eds.). Fürth: Filander Press, Germany.

[7] Layne, J.N., and M.A. Raymond (1994): Communal nesting of southern flying squirrels in Florida. *Journal of Mammalogy* 75: 110–120.

[8] Muul, I., (1962): Behavior of Michigan flying squirrels. *Jack-Pine Warbler* 40: 122–124.

[9] Muul, I., (1968): Behavioral and physiological influences on the distribution of the flying squirrel, *Glaucomys volans*. *University of Michigan, Museum of Zoology, Miscellaneous Publications* 134: 1–65.

[10] Nachtigall, W., (1979): Gleitflug des Flugbeutlers *Petaurus breviceps papuanus* II. Filmanalysen zur Einstellung von Gleitbahn und Rumpf sowie zur Steurung des Gleitflugs. *Journal of Comparative Physiology* A 133: 89–95.

[11] Nachtigall, W., R. Grosch, and T. Schultze-Westrum (1974): Gleitflug des Flugbeutlers *Petaurus breviceps papuanus* (Thomas): Flugverhalten und Flugsteuerung. *Journal of Comparative Physiology* 92: 105–115.

[12] Norberg, U.M., (1990): Gliding flight. In: *Zoophysiology 27, Vertebrate Flight: Mechanics, Physiology, Morphology, Ecology, and Evolution* (S.D. Bradshaw, W. Burggren, H.C. Heller, S. Ishii, H. Langer, G. Neuweiler, D.J. Randall, eds.). New York: Springer-Verlag, pp. 65–75.

[13] Polyokova, R.S., and A.S. Sokolov (1965): Structure of locomotor organs in the volant squirrel, *Pteromys volans* L. in relation to its plane flight. *Zoologichiski Zhurnal* 44: 902–916.

[14] Robins, J.H., (1994): Morphology and performance in the southern flying squirrel, *Glaucomys volans*. M.Sc. thesis, Southeast Missouri State University, Cape Girardeau, MO, USA.

[15] Robins, J.H., J.S. Scheibe, and K. Laves (this volume): Sexual size dimorphism and allometry in southern flying squirrels, *Glaucomys volans*. In: *The Biology of Gliding Mammals* (R.L. Goldingay & J.S. Scheibe, eds.). Fürth: Filander Press, Germany.

[16] Schaller, D., (1984): Wing evolution. In: *The Beginnings of Birds: Proceedings of the International Archaeopteryx Conference, Eichstatt.* (M.K. Hecht, J.H. Ostrom, G. Viohl and P. Wellnhofer, eds.). Willibaldsburg: Freunde des Jura-Musums Eichstatt, pp. 333–348.

[17] Scheibe, J.S., and J.H. Robins (1998): Morphological and performance attributes of gliding mammals. In: *Ecology and Evolutionary Biology of Tree Squirrels* (M.A. Steele, J.F. Merritt and D.A. Zegers, eds.). Virginia Museum of Natural History, Special Publication Vol. 6, pp. 131–144.

[18] Scholey, K., (1986): The climbing and gliding locomotion of the giant red flying squirrel, *Petaurista petaurista* (Sciuridae). *Biona-report* 5: 187–204.

[19] Sollberger, D.E., (1943): Notes on the breeding habits of the eastern flying squirrel (*Glaucomys volans volans*). *Journal of Mammalogy* 24: 163–173.

[20] Thorington, R.W. Jr., and L.R. Heaney (1981): Body proportions and gliding adaptations of flying squirrels (Petauristinae). *Journal of Mammalogy* 62: 101–114.

[21] Thorington, R.W. Jr., K. Darrow, and C.G. Anderson (1998): Wing tip anatomy and aerodynamics in flying squirrels. *Journal of Mammalogy* 79: 245–250.